How Bad Metals Turn Good: Spectroscopic Signatures of Resilient Quasiparticles

Xiaoyu Deng,[1,2,3] Jernej Mravlje,[4,1,5] Rok Žitko,[5] Michel Ferrero,[1] Gabriel Kotliar,[3] and Antoine Georges[4,1,6,2]

[1]*Centre de Physique Théorique, Ecole Polytechnique, CNRS, 91128 Palaiseau Cedex, France*
[2]*Japan Science and Technology Agency, CREST, Kawaguchi 332-0012, Japan*
[3]*Department of Physics, Rutgers University, Piscataway, New Jersey 08854, USA*
[4]*Collège de France, 11 place Marcelin Berthelot, 75005 Paris, France*
[5]*Jožef Stefan Institute, Jamova 39, Ljubljana, Slovenia*
[6]*DPMC, Université de Genève, 24 quai Ernest Ansermet, CH-1211 Genève, Suisse*

(Received 4 October 2012; published 19 February 2013)

We investigate transport in strongly correlated metals. Within dynamical mean-field theory, we calculate the resistivity, thermopower, optical conductivity and thermodynamic properties of a hole-doped Mott insulator. Two well-separated temperature scales are identified: T_{FL} below which Landau Fermi liquid behavior applies, and T_{MIR} above which the resistivity exceeds the Mott-Ioffe-Regel value and bad-metal behavior is found. We show that quasiparticle excitations remain well defined above T_{FL} and dominate transport throughout the intermediate regime $T_{\mathrm{FL}} \lesssim T \lesssim T_{\mathrm{MIR}}$. The lifetime of these resilient quasiparticles is longer for electronlike excitations and this pronounced particle-hole asymmetry has important consequences for the thermopower. The crossover into the bad-metal regime corresponds to the disappearance of these excitations and has clear signatures in optical spectroscopy.

DOI: 10.1103/PhysRevLett.110.086401 PACS numbers: 71.27.+a, 72.10.−d, 72.15.Jf, 78.20.−e

The transport properties of metals with strong electron correlations are unconventional and poorly understood theoretically. Two facts regarding the temperature dependence of the resistivity are frequently observed. (i) Fermi-liquid (FL) behavior $\rho \propto T^2$ only holds below a temperature T_{FL} which is low compared to bare electronic energy scales. (ii) At high temperatures, the resistivity is large and reaches values exceeding the Mott-Ioffe-Regel (MIR) value. This bad-metallic behavior [1] signals the breakdown of a quasiparticle (QP) description of transport, since the associated mean-free path l would be smaller than the lattice spacing. This is observed in many materials: Sr_2RuO_4 has $T_{\mathrm{FL}} \simeq 20$ K, while the MIR value is reached at $T_{\mathrm{MIR}} \simeq 800$ K (using $k_F l \sim 1$ as the MIR criterion); in LiV_2O_4, T_{FL} is a few degrees Kelvin, while T_{MIR} is several hundreds, etc. (see Refs. [2,3] for reviews). In two-dimensional organic materials, T_{FL} and T_{MIR} are closer but still distinct scales [4–6].

These observations raise the following questions. Why is T_{FL} much lower than T_{MIR} and what determines its value? Up to which temperature do QPs exist and what are the signatures of their disappearance? And, most importantly: how should one think of transport not only in the bad metal, but also in the intermediate regime $T_{\mathrm{FL}} \lesssim T \lesssim T_{\mathrm{MIR}}$ where the resistivity does not follow Landau's T^2 behavior, but is still smaller than the MIR value? These questions also apply to cuprate superconductors, where the observation of quantum oscillations [7,8] and T^2 behavior in transport [9,10] and optics [11] have rejuvenated the relevance of FL states with a low T_{FL} (possibly with angular dependence along the Fermi surface).

In this Letter, we answer these questions in a particularly simple setting: a hole-doped Mott insulator described with dynamical mean-field theory (DMFT). Our most striking finding is that well-defined QP excitations survive well above the range of validity of FL theory. Up to at least $10T_{\mathrm{FL}}$, the transport can be accurately described in terms of these resillient quasiparticles (RQPs). The high-temperature MIR crossover into the bad-metal regime is associated with their gradual extinction, which has a clear signature both in the single-particle spectral function and in optical spectroscopy. In a hole-doped Mott insulator, the RQPs come with a strong particle-hole asymmetry: electronlike excitations are longer-lived than holelike ones. This has direct consequences for the thermopower.

Previous DMFT work has investigated transport [12–16] and optical conductivity [6,17], but not the precise temperature-dependence of the self-energy and of the momentum-resolved spectral function which reveals this intermediate RQP regime. We note that in the half filled case relevant to organic compounds [4,5], the high-temperature state is insulatinglike, and hence, the temperature window where this regime can be seen is narrower.

We solved the DMFT equations [18] for the hole-doped Hubbard model using highly accurate numerical-renormalization group [19,20] and continuous-time quantum Monte Carlo [21,22] techniques. In DMFT, the real part of the optical conductivity reads

$$\sigma(\omega) = \frac{2\pi e^2}{\hbar} \int d\omega' F_{\omega,\omega'} \int d\varepsilon \Phi(\varepsilon) A_{\mathbf{k}}(\omega') A_{\mathbf{k}}(\omega' + \omega), \tag{1}$$

where $F_{\omega,\omega'} = [f(\omega') - f(\omega + \omega')]/\omega$ with $f(\omega)$ the Fermi function. $A_{\mathbf{k}}(\omega) = -(1/\pi)\mathrm{Im}[\omega + \mu - \varepsilon_{\mathbf{k}} - \Sigma(\omega)]^{-1}$ is

the single-particle spectral function, with $\varepsilon_{\mathbf{k}}$ the energy of the state in the band, $\Sigma(\omega)$ the retarded self-energy, and μ the chemical potential. $\Phi(\varepsilon) = (1/V)\sum_{\mathbf{k}}(\partial\varepsilon_{\mathbf{k}}/\partial\mathbf{k}_x)^2\delta(\varepsilon-\varepsilon_{\mathbf{k}})$ contains the information about velocities. We used a semicircular density-of-states (DOS) with a half-width D and the corresponding sum-rule preserving expression $\Phi(\varepsilon) = \Phi(0)[1-(\varepsilon/D)^2]^{3/2}$. In the following, resistivity will be expressed in units of the MIR value defined as $1/\rho_{\mathrm{MIR}} \equiv e^2\Phi(0)/\hbar D$. This choice is consistent with the criterion $k_F l = 1$ for a parabolic band in two dimensions, for which the conductivity $\sigma = (k_F l)e^2\Phi(\varepsilon_F)/\hbar\varepsilon_F = (k_F l)e^2/h$.

Figure 1(c) summarizes our main result: as a function of temperature, three distinct regions appear. At low $T < T_{\mathrm{FL}}$, FL behavior is found. At high temperature, the system is a bad metal with no quasiparticles [this is indicated by the shaded area on Fig. 1(c), more details below]. Between these two limits, there is an extended region with well-defined quasiparticles which, however, do not obey FL behavior. The nature of this metal with resilient quasiparticles (RQPs) is the central focus of our work.

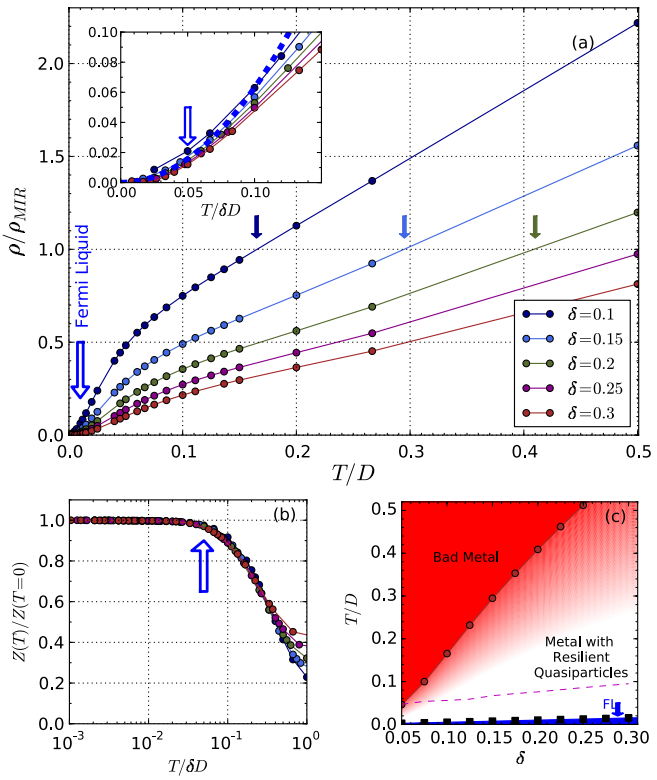

FIG. 1 (color online). (a) Temperature-dependence of the resistivity for several doping levels δ ($U/D = 4$, as in all figures). The MIR value as defined in the text is reached at a temperature T_{MIR} indicated by plain arrows. Inset: resistivity at low temperatures vs $T/\delta D$ revealing the T^2 behavior (dashed line) below T_{FL} (empty arrow). (b) Determination of T_{FL} by a scaling plot of $Z(T)/Z(T\to 0)$ vs $T/\delta D$. Here, $Z(T)^{-1} \equiv 1 - \partial \mathrm{Re}\Sigma(\omega, T)/\partial\omega$. (c) The different regimes: FL for $T < T_{\mathrm{FL}}$, bad-metal and intermediate RQP regime. The crossover into the bad metal is gradual: the onset of shading corresponds to the optical spectroscopy signatures discussed in the text, while the points indicate where ρ_{MIR} is reached. The thin dashed line indicates the knee in $\rho(T)$.

Let us first discuss transport [resistivity vs T, Fig. 1(a)] in the light of these regimes. At low temperature, the resistivity has a FL T^2 behavior. This extends up to a temperature T_{FL} [see inset in Fig. 1(a)] which is proportional to the doping level: $T_{\mathrm{FL}} \simeq 0.05\delta D$. Note that T_{FL} can be determined by other complementary criteria, like the scaling of $\mathrm{Im}\Sigma(\omega, T)/T^2$ vs ω/T (see Supplemental Material [23]) or the scaling of $Z(T=0)/Z(T)$ vs $T/\delta D$ [Fig. 1(b)]. Above T_{FL}, the resistivity increases approximately linearly (with a negative intercept). A kneelike feature is observed at a temperature T_*, above which the high-T regime gradually sets in. $\rho(T)$ then has a linear temperature dependence (with a positive intercept), as can be shown from a high-T expansion [15,16] and smoothly crosses ρ_{MIR} [see arrows in Fig. 1(a)] at a temperature $T_{\mathrm{MIR}} \sim 2\delta D$.

The data, therefore, show that there is a wide temperature range in which transport does not follow the T^2 FL behavior, although the resistivity is still substantially smaller than ρ_{MIR}. This raises the following question: what are the charge carriers in this intermediate metallic regime? To this aim, we depict in Fig. 2 the momentum-resolved spectral function $A_{\mathbf{k}}(\omega)$ at selected temperatures as energy distribution curves ($A_{\mathbf{k}}(\omega)$ vs ω for different $\varepsilon_{\mathbf{k}}$'s as well as the momentum-integrated DOS). These results reveal a remarkable fact: well-defined QP excitations exist throughout this intermediate regime, way above the FL scale. Our definition of the term "quasiparticle" is a pragmatic one: we mean that $A_{\mathbf{k}}(\omega)$ displays a well-resolved peak in the vicinity of the Fermi level, in addition to a lower Hubbard band (LHB) and an upper Hubbard band (UHB).

For $T < T_{\mathrm{FL}}$ ($T/D = 0.0025$ in Fig. 2), sharp peaks are seen close to the Fermi energy ($\omega = 0$), characteristic of long-lived Landau QPs. For $T > T_{\mathrm{FL}}$ ($T/D = 0.05$ curves), the peaks broaden and the RQPs are visible mostly on the unoccupied side of the Fermi surface ($\omega > 0$). As the temperature increases (see, e.g., $T/D = 0.2$), the QP can barely be resolved (see the Supplemental Material [23] for a color map representation) and eventually, disappear, with just the Hubbard satellites remaining in the spectra [e.g., the two-peak structure that is visible in the total DOS of Fig. 2(a) at $T/D = 0.2$ is not present for $T/D = 0.5$ anymore]. This crossover into the bad-metallic regime is a gradual one and there is not a precise temperature where the QP suddenly die out (below, we discuss how the optical conductivity provides a criterion for the onset of the bad-metallic behavior). Our data, nevertheless, clearly show that they still exist well above T_* and that they have completely disappeared at T_{MIR}.

T_{FL} and T_{MIR} appear as overall scales between which RQPs exist. Both these temperatures are proportional to the

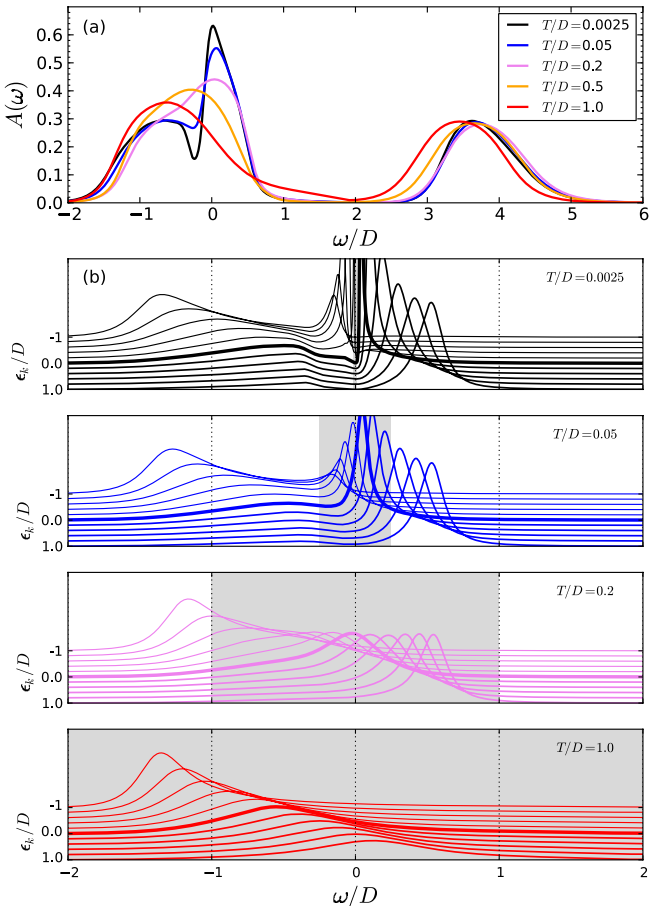

FIG. 2 (color online). (a) Temperature evolution of the total DOS for $\delta = 0.2$. (b) Momentum-resolved spectral functions. The shaded area $[-5k_BT, 5k_BT]$ indicates the states with a significant contribution to transport.

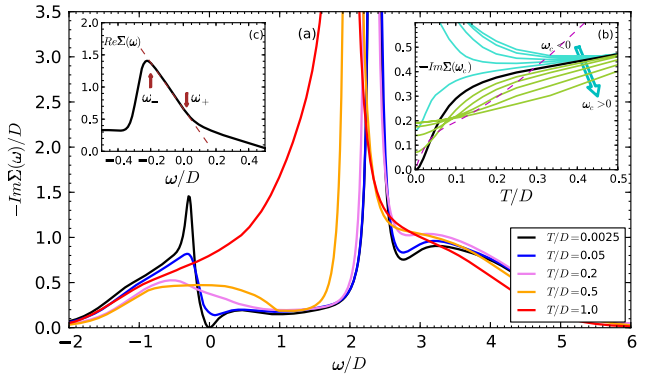

FIG. 3 (color online). Self-energy and particle-hole asymmetry. (a) $\mathrm{Im}\Sigma(\omega)$ for different temperatures. (b) Temperature dependence of $\mathrm{Im}\Sigma(\omega_c)$ for $\omega_c = -0.5, -0.4, \ldots, -0.1$, $\omega_c = 0.0$ (thick), and $\omega_c = 0.1, 0.2, \ldots, 0.5$. Below the dashed line $Z(T)\mathrm{Im}\Sigma \lesssim T$. (c) $\mathrm{Re}\Sigma(\omega)$ at $T/D = 0.0025$ and the two kinks (arrows).

doping level δ but with very different prefactors $T_{\mathrm{FL}}/T_{\mathrm{MIR}} \simeq 0.025$. Correspondingly, the resistivity at T_{FL} is much smaller than ρ_{MIR}, $\rho(T_{\mathrm{FL}})/\rho_{\mathrm{MIR}} \simeq 0.016$ [a low-T expansion in the FL region yields $\rho(T)/\rho_{\mathrm{MIR}} \sim 6.3(T/\delta D)^2 + \cdots$]. Let us emphasize that the Brinkman-Rice scale δD, which is a measure of the kinetic energy of QPs and hence, of the quantum degeneracy scale, is associated with T_{MIR}, not with T_{FL}.

Examination of the self-energy (Fig. 3) helps understanding the nature of the QP excitations as well as of the different transport regimes. In local DMFT, $-Z\mathrm{Im}\Sigma$ can be interpreted at low-ω as the inverse of the QP lifetime and $-\mathrm{Im}\Sigma$ as the transport scattering rate. Figure 3(b) displays $\mathrm{Im}\Sigma(\omega, T)$ vs T for different excitation energies ω. At $\omega = 0$ (thick curve), FL behavior $\mathrm{Im}\Sigma \sim T^2$ applies at low-T, corresponding to very long-lived QPs. Note that strict FL behavior breaks down already below the temperature at which $-Z\mathrm{Im}\Sigma(0, T) \sim T$ [24]. At finite frequency, the holelike excitations have higher scattering rate than electronlike ones [Figs. 3(a) and 3(b)]. At $T_* \simeq 0.08D$, the curves of $\mathrm{Im}\Sigma$ vs T for different positive ω's display a crossing point. Above T_*, the scattering rate is a decreasing function of frequency: low-energy electronlike excitations with finite $\omega > 0$ have a longer lifetime than those at $\omega = 0$. These finite-energy $\omega > 0$ excitations provide the largest contribution to conductivity in the intermediate RQP regime [25]. Their inverse lifetime depends weakly on temperature for $T > T_*$ [almost saturated behavior in Fig. 3(b)] and remains much smaller than the bandwidth and at most comparable to k_BT. For early considerations on a QP description of transport beyond the FL regime in the context of electron-phonon interactions, see Ref. [26].

The strong electron-hole asymmetry has also other interesting consequences. Because in the RQP regime the $\omega < 0$ states are strongly damped, the Fermi surface as determined by the maximum intensity of $A_{\mathbf{k}}(\omega = 0)$ inflates to a larger volume than the $T = 0$ Luttinger volume (see the Supplemental Material [23]). From Fig. 3(c), it is also seen that the deviation from linearity of $\mathrm{Re}\Sigma$ [$\sim \Sigma_0 + \omega(1 - 1/Z)$ at low ω] defines two distinct energy scales, $-\omega_-$ for holelike and ω_+ for electronlike excitations, leading to kinks in QP dispersions, as documented by previous studies [27,28]. We note that the smallest kink energy $\omega_+ \ll \omega_-$ sets the scale for deviations from FL behavior ($\omega_+ \simeq \pi T_{\mathrm{FL}}$). Using quite different theoretical methods, previous studies [29,30] have also emphasized the importance of particle-hole asymmetry in hole-doped Mott insulators.

A sensitive probe of the particle-hole asymmetry is the Seebeck coefficient (thermopower) $Q(T)$ shown on Fig. 4. Strikingly, the subleading particle-hole asymmetric terms in the low-frequency expansion of $\mathrm{Im}\Sigma$ modify the slope of $Q(T)$ at low-T by a factor of about 2, as compared to a naive FL theory estimate (thick dashed line) that would only retain terms $\sim \omega^2 + (\pi T)^2$. This effect was anticipated in Ref. [31] and is shown here to be quantitatively important. The near saturation of the scattering rate of the

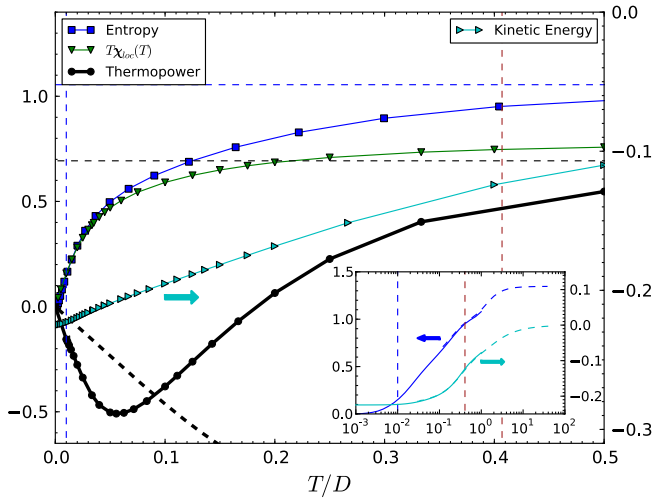

FIG. 4 (color online). Entropy (in units of k_B), $T\chi_{\rm loc}$ ($\mu_B = 1$), and Seebeck coefficient (in units of $k_B/|e|$) for $\delta = 20\%$. Horizontal dashed lines indicate the atomic (Heikes) limit for the entropy and thermopower. Vertical dashed lines denote $T_{\rm FL}$ and $T_{\rm MIR}$. The thermopower at low-T is compared to the FL estimate (thick dashed) in which the particle-hole asymmetry of $\mathrm{Im}\Sigma$ is neglected. Kinetic energy in units of D (right scale). Inset: Entropy and kinetic energy versus temperature on a log scale.

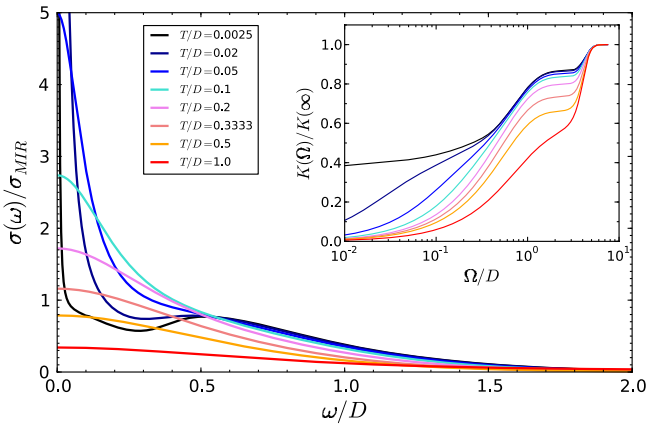

FIG. 5 (color online). Optical conductivity for $\delta = 20\%$. Inset: optical spectral weight integrated up to Ω, normalized to the kinetic energy.

RQPs, discussed above, is also responsible for $Q(T)$ still increasing in an electronlike manner up to $T \simeq T_*$. At a higher temperature within the RQP regime, $Q(T)$ changes sign and, when entering the bad-metal regime, approaches the simple Heikes estimate for $D \lesssim T \ll U$ (Fig. 4). The atomic Kelvin formula [23,32] successfully describes the thermopower there, which can, thus, be taken as another fingerprint of a bad metal. The accuracy of approximate formulas for thermopower has been tested also in other studies [33,34].

It is interesting to observe how the different transport regimes relate to thermodynamic observables. On Fig. 4, we display the entropy $S(T)$, the kinetic energy $K(T)$, and the Curie constant $T\chi_{\rm loc}$ associated with the local ($\mathbf{q}$-integrated) magnetic susceptibility. The entropy as well as the Curie constant reach remarkably high values already below $T_{\rm MIR}$. In the RQP regime, the system, thus, has to be thought of in terms of two fluids: a mixture of local moments and of the resilient QP states. Above $T_{\rm MIR}$, the entropic contribution to the free energy overcomes the kinetic energy gain. The system is fully incoherent, its entropy approaches the atomic limit, and the Curie constant saturates.

Optical spectroscopy (Fig. 5) can be used to detect the two crossovers, between the FL and the RQP regime and from the latter into the bad metal. For $T < T_{\rm FL}$, $\sigma(\omega)$ displays a narrow low-frequency peak which decays as $1/\omega^2$. This Drude peak corresponds to optical transitions involving only QP states and has a spectral weight proportional to doping level δ. In the FL regime, the Drude peak is well separated from a higher frequency hump (at $\omega/D \sim 0.5$ in Fig. 5) which corresponds to transitions between the LHB and QP states [17]. The distance of the LHB to the Fermi level, of order μ (a fraction of the bandwidth) sets the energy scale for these transitions. This typically corresponds to the midinfrared range in narrow band correlated materials. The crossover out of the FL regime into the resilient metal regime leads to a broader low-frequency peak whose frequency dependence is no longer $1/\omega^2$. For $T/D = 0.02$, $\sigma(\omega)$ can be fit to $1/\omega^\alpha$ with $\alpha \approx 1.2$ for frequencies $0.02 \lesssim \omega/D \lesssim 0.2$. The low-$T$ data display an interesting non-Drude foot with a weak frequency dependence of $\sigma(\omega)$ between the Drude and the midinfrared peaks. Above T_*, the Drude and midinfrared features merge.

For a rather extended temperature range into the RQP regime, the spectral weight redistribution upon increasing T takes place essentially entirely between the low-energy QP states and the midinfrared feature, see inset of Fig. 5. For $T \gtrsim T_*$ (warmer part of the intermediate regime), some spectral weight transfer to higher frequencies starts taking place as well.

The beginning of the crossover into the bad-metal regime is signaled by two changes in $\sigma(\omega)$ happening at the same temperature of order δD [it is shown as the onset of shading in Fig. 1(c), which allows us to have a clear view of the region where well-defined quasiparticles exist]. First, the isosbestic crossing point (at $\omega/D \simeq 0.5$) is lost and the low-frequency non-Drude peak is replaced by a very broad peak, which corresponds to transitions involving only the LHB. Second, spectral weight is now redistributed over a considerable energy range, extending all the way to the UHB (inset). In the bad metal, the kinetic energy [to which $\sigma(\omega)$ integrates] is strongly dependent on temperature (Fig. 4) and the broad peak has, correspondingly, a height which continues diminishing with T, which implies that the resistivity does not saturate [2].

In summary, our study reveals that resilient QP excitations persist well above T_{FL}. They control transport properties until they disappear at a temperature roughly of order T_{MIR}. The coexistence of QP states with localized magnetic moments which carry large entropy is intriguing and demands closer theoretical investigation including antiferromagnetic correlations beyond DMFT. For hole-doped Mott insulators, a pronounced particle-hole asymmetry is found. This calls for new momentum-resolved spectroscopic probes which would be able to access the dark side of the Fermi surface and for closer investigations of the electron-doped materials where the signatures of this regime could be seen using conventional angle-resolved photoemission spectroscopy.

We would like to thank C. Berthod, L. de' Medici, M. Dressel, A. Millis, T. V. Ramakrishnan, A. M. Tremblay, D. van der Marel, and especially, N. Hussey and S. Shastry for very useful discussions, and Wenhu Xu for exchanges about thermodynamic observables. This work was partially supported by ICAM (X. D.) and the Swiss National Science Foundation MaNEP program. R. Ž. was supported by ARRS under Program No. P1-0044.

Note added.—During completion of this manuscript, related results regarding the thermopower were independently reported [35].

[1] V. J. Emery and S. A. Kivelson, Phys. Rev. Lett. **74**, 3253 (1995).
[2] N. Hussey, K. Takenaka, and H. Takagi, Philos. Mag. **84**, 2847 (2004).
[3] O. Gunnarsson, M. Calandra, and J. E. Han, Rev. Mod. Phys. **75**, 1085 (2003).
[4] J. Merino and R. H. McKenzie, Phys. Rev. B **61**, 7996 (2000).
[5] P. Limelette, P. Wzietek, S. Florens, A. Georges, T. A. Costi, C. Pasquier, D. Jérome, C. Mézière, and P. Batail, Phys. Rev. Lett. **91**, 016401 (2003).
[6] J. Merino, M. Dumm, N. Drichko, M. Dressel, and R. H. McKenzie, Phys. Rev. Lett. **100**, 086404 (2008).
[7] N. E. Hussey, M. Abdel-Jawad, A. Carrington, A. P. Mackenzie, and L. Balicas, Nature (London) **425**, 814 (2003).
[8] N. Doiron-Leyraud, C. Proust, D. LeBoeuf, J. Levallois, J.-B. Bonnemaison, R. Liang, D. A. Bonn, W. N. Hardy, and L. Taillefer, Nature (London) **447**, 565 (2007).
[9] N. E. Hussey, J. Phys. Condens. Matter **20**, 123201 (2009).
[10] M. Greven and N. Barišić (private communication).
[11] S. I. Mirzaei, D. Stricker, J. N. Hancock, C. Berthod, A. Georges, E. van Heumen, M. K. Chan, X. Zhao, Y. Li, M. Greven, N. Barišić, and D. van der Marel, arXiv:1207.6704.
[12] T. Pruschke, D. Cox, and M. Jarrell, Europhys. Lett. **21**, 593 (1993).
[13] M. Jarrell and T. Pruschke, Phys. Rev. B **49**, 1458 (1994).
[14] H. Kajueter, G. Kotliar, and G. Moeller, Phys. Rev. B **53**, 16214 (1996).
[15] G. Pálsson and G. Kotliar, Phys. Rev. Lett. **80**, 4775 (1998).
[16] G. Palsson, Ph.D. thesis, Rutgers University, 2001.
[17] M. Jarrell, J. K. Freericks, and T. Pruschke, Phys. Rev. B **51**, 11704 (1995).
[18] A. Georges, G. Kotliar, W. Krauth, and M. J. Rozenberg, Rev. Mod. Phys. **68**, 13 (1996).
[19] R. Bulla, T. A. Costi, and T. Pruschke, Rev. Mod. Phys. **80**, 395 (2008).
[20] R. Žitko, http://nrgljubljana.ijs.si/.
[21] E. Gull, A. J. Millis, A. I. Lichtenstein, A. N. Rubtsov, M. Troyer, and P. Werner, Rev. Mod. Phys. **83**, 349 (2011).
[22] M. Ferrero and O. Parcollet, http://ipht.cea.fr/triqs.
[23] See Supplemental Material at http://link.aps.org/supplemental/10.1103/PhysRevLett.110.086401 for for the FL scaling of the self-energies, the color maps of the momentum-resolved spectral functions, the inflation of the Fermi surface, the temperature dependence of the chemical potential, and the high-temperature behavior of the Seebeck coefficient.
[24] J. Mravlje, M. Aichhorn, T. Miyake, K. Haule, G. Kotliar, and A. Georges, Phys. Rev. Lett. **106**, 096401 (2011).
[25] For $T \lesssim T_{\mathrm{MIR}}$, the dc conductivity from Eq. (1) can be approximated by a generalized Drude-like formula, $\sigma_{dc} \propto \int d\omega f'(\omega)\Phi(\epsilon^*_{\omega,T})/\mathrm{Im}\Sigma(\omega)$, with $\epsilon^*_{\omega,T} \equiv \mu + \omega - \mathrm{Re}\Sigma$. This approximation is highly accurate up to T_*. The $\omega > 0$ range provides the largest contribution in the RQP regime.
[26] R. E. Prange and L. P. Kadanoff, Phys. Rev. **134**, A566 (1964).
[27] K. Byczuk, M. Kollar, K. Held, Y.-F. Yang, I. A. Nekrasov, T. Pruschke, and D. Vollhardt, Nat. Phys. **3**, 168 (2007).
[28] P. Grete, S. Schmitt, C. Raas, F. B. Anders, and G. S. Uhrig, Phys. Rev. B **84**, 205104 (2011).
[29] M. M. Zemljič, P. Prelovšek, and T. Tohyama, Phys. Rev. Lett. **100**, 036402 (2008).
[30] B. S. Shastry, Phys. Rev. Lett. **109**, 067004 (2012).
[31] K. Haule and G. Kotliar, in *Properties and Applications of Thermoelectric Materials*, edited by V. Zlatić and A. C. Hewson NATO Science for Peace and Security Series B: Physics and Biophysics (Springer Netherlands, Dordrecht, 2009), p. 119.
[32] M. R. Peterson and B. S. Shastry, Phys. Rev. B **82**, 195105 (2010).
[33] M. Uchida, K. Oishi, M. Matsuo, W. Koshibae, Y. Onose, M. Mori, J. Fujioka, S. Miyasaka, S. Maekawa, and Y. Tokura, Phys. Rev. B **83**, 165127 (2011).
[34] W. Xu, C. Weber, and G. Kotliar, Phys. Rev. B **84**, 035114 (2011).
[35] L.-F. Arsenault, B. S. Shastry, P. Sémon, and A.-M. S. Tremblay, arXiv:1209.4349.